The atmospheric boundary layer and surface conditions during katabatic wind events over the Terra Nova Bay Polynya.

M. Wenta[1], J. J. Cassano[2]

[1]Institute of Oceanography, University of Gdansk, Poland
[2]Cooperative Institute for Research in Environmental Sciences and Department of Atmospheric and Oceanic Sciences, University of Colorado, Boulder, CO, USA

Key Points:

- atmospheric boundary layer
- sea ice–atmosphere interactions
- katabatic winds

Corresponding author: Marta Wenta, marta.wenta@phdstud.ug.edu.pl

Abstract

Off the coast of Victoria Land, Antarctic an area of open water - the Terra Nova Bay Polynya (TNBP)- persists throughout the austral winter. The primary force driving the development of this almost ice-free stretch of water are extreme katabatic winds flowing down the slopes of Transantarctic Mountains. The surface-atmosphere coupling and ABL transformation during the katabatic flow between 18-25 September 2012 in Terra Nova Bay are studied, using observations from Aerosonde unmanned aircraft system (UAS) observations, numerical modeling results and Antarctic Weather Station (AWS) measurements. Our analysis demonstrates that the intensity and persistence of katabatic winds is governed by sea level pressure (SLP) changes in the region. Whereas the duration and intensity of the flow, determines the polynya extent. When cold, dry air brought with the winds interacts with relatively warm surface of the polynya the convection starts to develop and overcomes the previously stable atmosphere. In general, the intensity of the flow, surface conditions in the bay and regional SLP fluctuations are all interconnected and together modify local atmospheric and surface conditions. The importance of valid forecast of katabatic events for Antarctic aircraft operations is unambiguous. The Antarctic Mesoscale Prediction System (AMPS) performs this task well, but due to exaggerated sea ice concentrations (SIC) incorrectly represents vertical ABL properties and air mass modification over the TNBP. Altogether, this research provides a unique description of TNBP development and its interactions with the atmosphere and katabatic winds, thus enhancing our understanding of the complex processes taking place in this region.

1 Introduction

Terra Nova Bay is located in the western Ross Sea, between Cape Washington in the North and the Drygalski Ice Tongue in the south, along the coast of Victoria Land, Antarctica. A notable characteristic of this area is the persistence of an ice-free sea throughout the winter – the Terra Nova Bay Polynya (TNBP), forced by the sea ice removal from the coast by strong offshore katabatic winds and maintained due to the presence of Drygalski Ice Tongue, which blocks the transport of ice from the south (Kurtz & Bromwich, 2013). The extent of the recurring polynya is defined by the distance between open water with frazil ice formation near the coast and the downwind area where the ice becomes compact. During winter the mean area occupied by the TNBP varies between 1000-1300 km^2 (VanWoert, 1999), but some observations indicate that it can reach even 8500 km^2(Ciappa et al., 2012).

Katabatic surface winds are generated over the interior of the Antarctic by intensive radiative cooling which is responsible for the development of near-surface inversion layer. The cold, negatively buoyant air is driven downslope through the valleys of Transantarctic Mountains, mainly due to combined thermodynamic and topography forcing. In the coastal area near the Terra Nova Bay the primary and wider route of flow descent is Reeves Glacier and the secondary one is the Priestly Glacier (Bromwich, 1989; Knuth. & Cassano, 2011) Fig.(1). Once the katabatic flow reaches the shore it spreads laterally over the ocean and can propagate over a long distance depending on the large-scale pressure field. The presence of relatively warm open water on the path of the cold katabatic wind, results in strong coupling between the surface and the overlying atmosphere and, in consequence, downward transfer of momentum, along with intensive, upward exchange of heat and moisture (Parish & Bromwich, 1989). As the energy from the surface is absorbed by the atmosphere the formation of new sea ice takes place, which is then transported further away from the coast by the offshore winds and currents. A continuous formation of sea ice and resulting rejection of salt increases the density of near–surface water (Minnett & Key, 2007) and produces the densest water in the ocean- the Antarctic Bottom Water (AABW). Studies indicate that TNBP may contribute about 10% of all AABW formed in the Ross Sea (VanWoert, 1999) and therefore plays a crucial role in the global termohaline circulation.

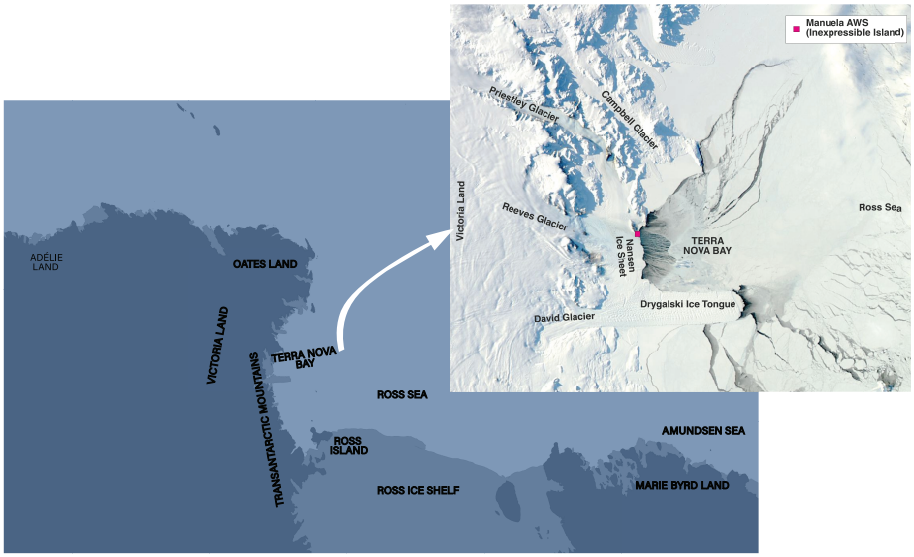

Figure 1. Map of Terra Nova Bay area. Satellite image for 20 of September 2012 from the NASA Worldview application (https://worldview.earthdata.nasa.gov), part of the NASA Earth Observing System Data and Information System (EOSDIS).

The intensity of the katabatic winds in Terra Nova Bay depends largely on the pressure gradient between the slopes and open sea, governed by large scale atmospheric circulation. The passage of low pressure system in the Ross Sea or presence of a cyclone to the east of Terra Nova Bay enhances the gradient and thus strengthens the winds, at the same time extending the duration of their influence on the atmosphere further away from the coast (Petrelli et al., 2008; Bromwich, 1989). On the other hand, observational and modelling studies indicate that the extent of the polynya is not only determined by the intensity and persistence of the katabatic winds but also the concentration of the pack ice outside of the polynya (Martin et al., 2001). Therefore, as we add to those factors an essential, blocking effect of Drygalski Ice Tongue, the opening and lifetime of the polynya depends on the range of oceanographic, meteorological and geographical conditions.

First reports about strong, persistent winds blowing in the Terra Nova Bay come from the journals of the Northern Party of Robert F. Scott's Terra Nova Expedition, which was stranded at the area throughout the winter (Bromwich & Kurtz, 1982). Further observations of extreme katabatic events in the Terra Nova Bay were largely limited to the summer season, as harsh, austral winter conditions of the Antarctic coast present a challenging environment for field campaigns. In consequence, scientists turned their attention toward satellite based studies (Kurtz & Bromwich, 1983; Ciappa et al., 2012; Parish & Bromwich, 1989) and numerical modelling (VanWoert, 1999; Petrelli et al., 2008; Morelli & Parmiggiani, 2013). The first observations of the atmospheric boundary layer (ABL) over the polynya were made with manned aircraft in late 80's (Parish & Bromwich, 1989). Since then a number of campaigns covering different branches of science have taken place in the bay, including studies of atmospheric chemistry (Sprovieri et al., 2002), seawater chemistry (Vecchiato et al., 2017), biology (Pane et al., 2004) and physical oceanography (Manzella et al., 1999). The first late winter measurements of the atmosphere and surface state in Terra Nova Bay have been done in September 2009 by Aerosonde unmanned aerial systems (UAS) (Knuth et al., 2013) and were followed up by a second successful Aerosonde UAS field campaign in September 2012 (Cassano et al., 2016), which provided a comprehensive three-dimensional description of the atmosphere over Terra Nova Bay during the occurrence of the polynya. Nevertheless, all of mentioned obser-

vations are limited to short periods of time and for now, the only source of continuous meteorological data from the coastal area of the bay are Antarctic Weather Stations (AWS) installed in the region in the 1980's and maintained by the cooperative efforts of the University of Wisconsin and other partners (Lazzara et al., 2012).

In this study the surface and atmospheric conditions in Terra Nova Bay between 13 and 25 September 2012 are analysed based on the numerical modelling simulations, satellite images and in-situ atmospheric measurements. The results of numerical weather prediction (NWP) simulations are obtained from the Antarctic Mesoscale Prediction System (AMPS) (Powers et al., 2003), which is a real–time Polar WRF forecasting system run over Antarctica, and from Modern-Era Retrospective analysis for Research and Applications (MERRA). Satellite images of sea ice concentration (SIC) come from the AMSR-E sensor (Spreen et al., 2008) and ice surface temperature (IST) from Visible Infrared Imager Radiometer Suite (VIIRS) (Tschudi et al., 2017). The continuous measurements of meteorological parameters in the upwind part of the bay are obtained from the Manuela AWS station located on the Inexpressible Island Fig.(1). The key element of presented research are UAV observations from September 2012 (Cassano et al., 2016)–the only source of data about atmospheric conditions above polynya. Wind speed and temperature measured during simultaneous flights in both downwind and cross wind directions are analysed in relation to surface sea ice concentration and temperature. Both UAS Aerosonde and and Manuela AWS observations are also used for the validation of AMPS model predictions. Furthermore, large scale fluctuations of sea level pressure (SLP) are considered to investigate the influence of synoptic conditions on the frequency of extreme katabatic exevents. Altogether, the purpose of our study is to provide a detailed description of the TNBP surface and atmospheric state during and between the polynya events, along with a short analysis of the AMPS model results.

2 Data and Methods

2.1 UAV Flights

The Aerosonde UAS is a small (3.6 m wingspan, 19–21 kg take-off weight), robotic, pusher-prop aircraft capable of carrying a variety of instrument packages and performing well in polar winter conditions. Throughout the analyzed flights it was equipped with the sensors to measure air temperature, relative humidity, atmospheric pressure and surface temperature. The wind speed and wind direction were calculated indirectly, based on the measurements from the UAS Piccolo Avionics system indicating the flight heading and speed. Detailed technical description of the aircraft and its capabilities can be found in Cassano et al. (2016). During the campaign in 2012 9 missions were flown from McMurdo Station, Antarctica to Terra Nova Bay on the 13, 18, 19, 22 and 25 of September. On those days, once the Aerosonde UAS flew past the Drygalski Ice Tongue the flight height was lowered to approximately 100-150 m and the measurement phase of the flight over TNBP began. The flight patterns above TNBP can be divided into two types (e.g. Fig. 2). The goal of the first one was to sample the downstream evolution of the air mass coming off the continent as the aircraft passed over the bay. Those downwind transects included repeated profiles of the atmosphere, made by the aircraft ascending and descending in the spiral pattern, from approximately 100 m to the top of the ABL. The aim of the second type of flight was to measure crosswind variability of the atmospheric state over TNBP. Therefore, the Aerosonde UAS flew in horizontal lines, roughly perpendicular to the low level flow, moving away from the coast with every new line. Spiral profiles were flown at the beginning, approximately at mid-point and at the end of each of these cross-wind legs. On the 13 of September the flight was short and included only a few horizontal transects. On 18, 19, 22 and 25 of September both the crosswind and downwind transects were flown above the surface of Terra Nova Bay, including repeated, second downwind transects conducted in order to sample the changes in the atmospheric state after a few hours. The analysis presented in this article focuses on the UAV ob-

servations of wind speed, wind direction and temperature with an emphasis on the vertical profiles observed during the Aerosonde flights.

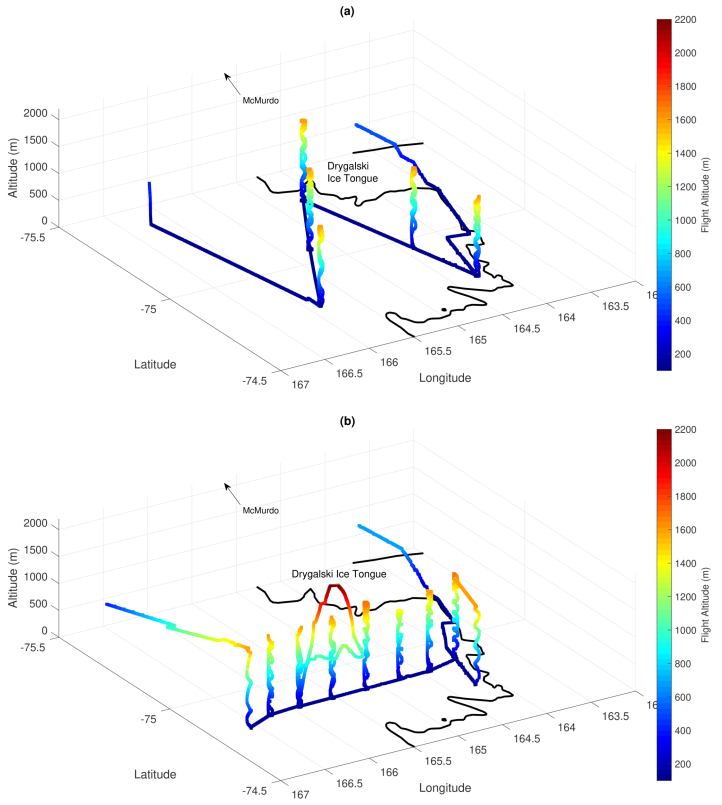

Figure 2. UAS Aerosonde crosswind (a) and transect (b) flights on the 25 of September 2012.

2.2 Manuela AWS

Manuela AWS is a part of the University of Wisconsin AWS network collecting meteorological data from a number of locations in the Antarctic (Lazzara et al., 2012). This AWS station on Inexpressible Island (74.96 S, 163.7 E) has been in operation since 1984. Sensors of air temperature, relative humidity, atmospheric pressure, wind speed and direction are mounted on the 3 m tower. The accuracy of the sensors is, approximately: $\pm$ 0.5 ^{o}C for temperature, $\pm$ 0.1 hPa for pressure,$\pm$ 2% for humidity,and $\pm$ 2% for wind speed and direction. Measurements are transmitted hourly via the ARGOS network and subjected to a quality control by the University of Wisconsin. The results, for the studied period, are provided in 1 hour intervals. Wind speed and direction, along with temperature observations from the station are analysed for the description of the upwind conditions during katabatic winds events.

2.3 Satellite Data

Satellite images of sea ice concentration and ice surface temperature provide us with a detailed description of surface conditions and enable an analysis of surface-atmosphere coupling in the Terra Nova Bay.

2.3.1 Sea Ice Concentration

Sea ice concentration images provided by the Institute of Environmental Physics, University of Bremen (Spreen et al., 2008) (`https://seaice.uni-bremen.de/sea-ice-concentration-amsr-eamsr2/`) are calculated daily, in near real time, from the AMSR2 sensor data. AMSR2, a successor of AMSR-E(Advanced Microwave Scanning Radiometer for EOS) is carried by the "Shizuku" (GCOM-W1) satellite, launched on May 18, 2012 and delivering data since August 2012. The frequency used for the calculation of SIC from brightness temperature is 89 GHz and the images are retrieved with the ARTIST Sea Ice (ASI) algorithm (Spreen et al., 2008). All swatch SIC data of one calendar day are re-sampled into various polar stereographic grids using the *near neighbour* routine. The regional maps, including the one for the area of Ross Sea, have a grid spacing of 3.125 km.

The approximate area of the polynya is calculated based on the maps of SIC. First, the gray colored maps of SIC below 70 % in Terra Nova Bay are generated and then the program Pixie is called to determine the spatial extent of the polynya. Pixie is a program created for the image analysis and available for free on GitLab (`https://gitlab.com/seadata-software/pixie`). It is a python script that applies simple methods of image recognition for given color intensity threshold, from 0 (black) to 255 (white). For the presented study, to calculate spatial coverage of all pixels present in gray colored maps, a threshold of 254 has been determined as the most suitable and applied for all images. Based on the computed number of classified pixels and the number of pixels present in the whole image, the total area of SIC below 70% in km^2 is computed. The value of 70% have been chosen based on the comparative analysis of IST and SIC images and similar studies of spatial polynya coverage (Parmigianni, 2011; Massom et al., 1998; Adams et al., 2011). It has to be noted that it is a rough estimation of polynya spatial extent, created to illustrate the changes in SIC with different synoptic and regional atmospheric conditions.

2.3.2 Ice Surface Temperature

Ice surface temperature data come from the radiance data acquired by the Visible Infrared Radiometer Suite (VIIRS) and processed by the NASA Goddard Space Flight Center (Tschudi et al., 2017). The VIIRS instrument flies on board the Suomi National Polar-orbiting Partnership (NPP) satellite. The VIIRS sea IST is computed from bands M15(10.763 μm) and M16(12.013 μm) of brightness temperature, using the split window method of Yu and Rothrock (1996). A reported accuracy of the applied algorithm (Key et al., 2013) is $\pm$ 1K. The presence of cloud cover or melt ponds and leads in the summer season may cause erroneous interpretation of the surface, however in the case considered in this article they are both either scarce or absent (winter season). Datasets with a spatial resolution of 750 m are provided at least daily, but for the areas were swaths overlap (near poles), may appear more frequently. For the considered period at least one image, without or with minimal clouds obstruction, is available for further analysis.

2.4 Numerical Modelling Results

2.4.1 Antarctic Mesoscale Prediction System

AMPS is a real time mesoscale modelling system providing numerical forecasts for the Antarctic since 2000 (Powers et al., 2001). It is run at the Mesoscale and Microscale Meteorology (MMM) Division of the National Center for Atmospheric Research (NCAR). In the period considered in our research AMPS used a Polar WRF Model version 3.2.1., developed at the Byrd Polar and Climate Research Center at Ohio State University. The model was initialized twice a day, at 0000 and 1200 UTC. For the western Ross Sea the horizontal resolution was 5 km. The boundary conditions were assimilated by the WRF

Data Assimilation System (WRFDA) with a three dimensional variational data assimilation (3DVAR) approach from the output of NCEP Global Forecast System (GFS; (Center, 2003)). Sea ice concentration is specified from daily SSM/I data. More detailed description of this version of the AMPS and the Polar WRF set-up for the Antarctic are available in Bromwich et al. (2013). The goal of the presented study is to evaluate part of the AMPS output, in particulate wind speed, direction and air temperature, in relation to the UAVs measurements and satellite images during the extreme katabatic events over the TNBP.

2.4.2 MERRA Reanalysis

The Modern-Era Retrospective analysis for Research and Applications (MERRA) data spans the period between 1979 and February 2016, thus covering the modern satellite era. The MERRA dataset was created with version 5.2.0 of the Goddard Earth Observing System (GEOS) atmospheric model and data assimilation system (DAS). The horizontal resolution of the output is 0.5^o x 0.66^o with 72 vertical layers. MERRA provides scientists with a state-of-art global analysis, with a focus on improved estimates of the global hydrological cycle. Furthermore, MERRA puts the observations from NASA's Earth Observing System (EOS) satellites into a climate context (Rienecker et al., 2011). In our analysis MERRA output is used for the investigation of synoptic scale sea level pressure changes in the Ross Sea during the UAS flights presented here.

3 Synoptic overview of the Ross Sea and Terra Nova Bay region

Regional scale circulation near Terra Nova Bay is dominated by the Amundsen Sea Low (ASL), a permanent region of low pressure located in the South Pacific sector of the Southern Ocean, which comprises the Ross Sea, Amundsen Sea and the Bellingshausen Sea. This region, including the Ross Sea (Carrasco & Bromwich, 1993) and Adélie Land (Bromwich et al., 2011) in particular, is known for significant cyclone activity due to the interaction of cold, dry continental air with relatively warm, moist air from Southern Ocean. The large scale winter atmospheric circulation in this region is characterized by alternating low and high pressure systems forming in the lower latitudes (60–70° S). The dominating direction of surface flow off the coast of Victoria Land is to the north, the intensity of the flow is defined by the surface pressure difference between the Ross Ice shelf and ASL. The katabatic flows off the continent and the development of mesoscale cyclones offshore may modify this pattern, especially during the winter season. Studies indicate that the presence of a synoptic cyclone in the eastern part of Ross Sea with isobars parallel to Transantarctic Mountains results in the generation of the katabatic events in Ross Ice Shelf and Terra Nova Bay (Seefeldt et al., 2007).

Figure 3 shows the evolution of SLP in the Ross Sea region throughout the period of 18-25 September 2012. During this time the sea level pressure (SLP) in the Ross Sea was dominated by the strong cyclone located near Marie Byrd Land (Fig.3, a–b). The pressure in the center of this extensive low was 940 hPa, while the Manuela AWS sensors measured 965 hPa. The large pressure gradient, together with isobars parallel to the Victoria Land resulted in the intensification of downslope and offshore flow, with wind speeds of up to 35 m/s in the upwind area of the Terra Nova Bay. During the following days between 20 and 22 of September the cyclone moved further toward the east, with decreasing influence on the Ross Sea SLP (Fig.3, c–e). Reanalysis results indicate that during that time a small low pressure system approached from the north and maintained a pressure difference above 10 hPa between the slopes of Transantarctic Mountains and central Ross Sea. During that time the strong winds persisted and the polynya remained open with an area of SIC lower than 70% covering 2838 km^2 on 22 of September. As the cyclone moved further to the east, an anticyclone approached from north-west and increased the SLP in the region up to 998-1000 hPa over the Ross Sea and almost 1000

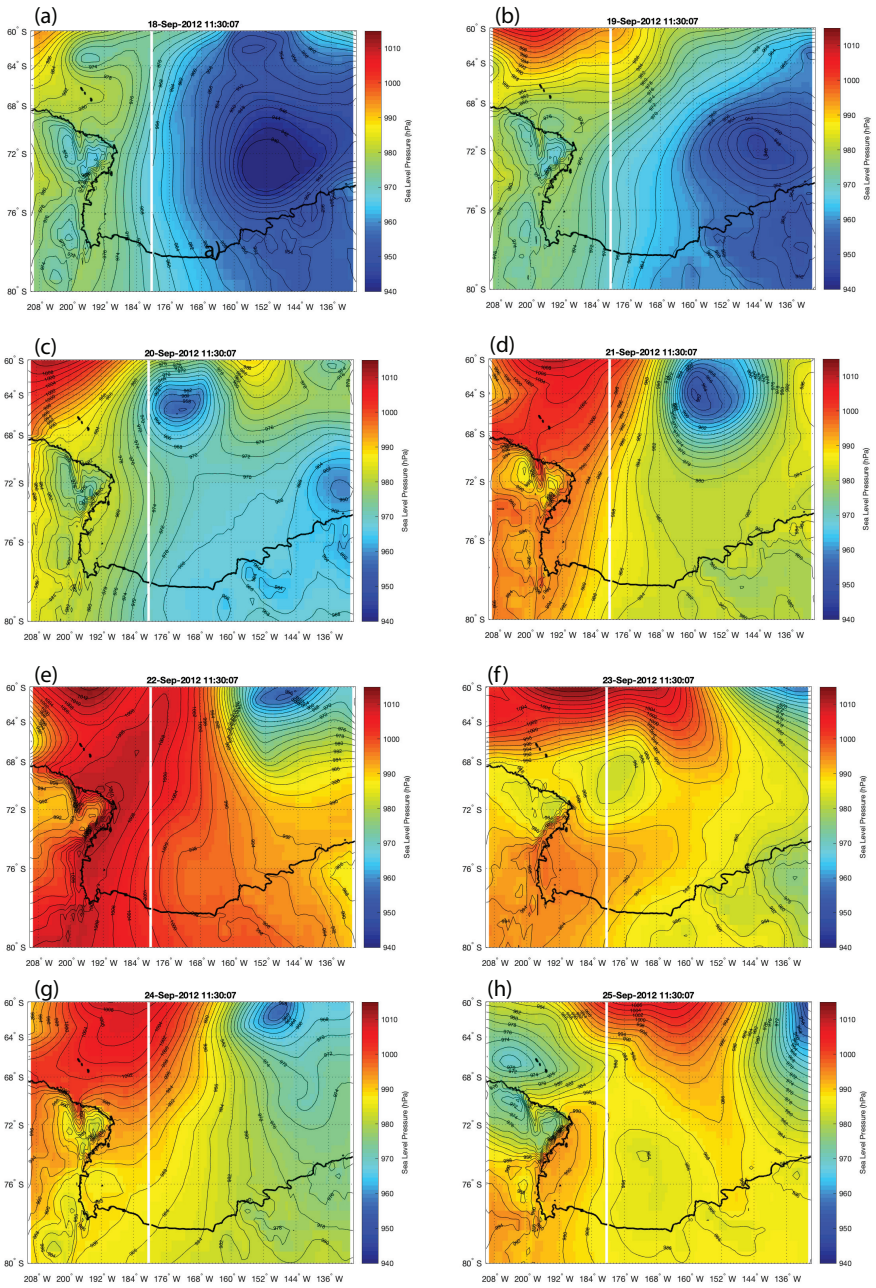

Figure 3. Sea level pressure maps for the Ross Sea area from MERRA dataset. Every image represents situation from a single hour of 11.30 am on a consecutive days between 18-25 September 2020.

hPa at the Manuela AWS (Fig.3, e–f). In consequence the pressure difference between the slopes near Terra Nova Bay and offshore sea weakened significantly and the wind speed decreased considerably on the 23 of September. Under those circumstances the wind speed decreased and the polynya closed and only a small patch of 53 km^2 of low SIC remained in the Terra Nova Bay. On the following days the high pressure system retreated to the north and a small cyclone appeared offshore of Oates Bank thus again increasing the pressure gradient between the slopes of Transantarctic Mountains and central Ross Sea to

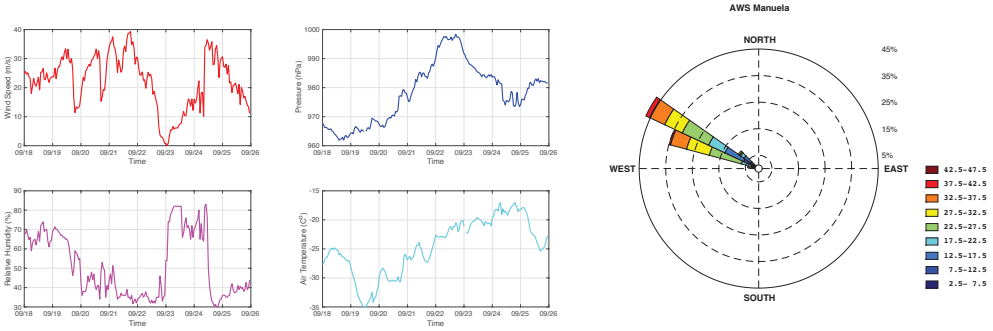

Figure 4. Measurements from Manuela AWS for the period of 18-25 September 2012 (`http://amrc.ssec.wisc.edu`).

approximately 10 hPa. Consequently, SIC in the Terra Nova Bay decreased again and the polynya opened reaching the size of 2407 km^2 on the 25 of September (Fig.3, g–h).

The magnitude of the pressure gradient between the slope of Transantarctic Mountains and Ross Sea surely affects the frequency and intensity of the katabatic winds, and through that the size of the polynya. However, the balance between the ice production in the open water zone and the movement of the offshore pack ice out of the Terra Nova Bay determines the total area of TNBP. The understanding of associated processes requires, among others, studies of dynamic and thermodynamic processes in sea ice and the oceanic mixed layer, which determine spatiotemporal changes in sea ice concentration, thickness and drift velocities. They are beyond the scope of this study.

3.1 Upwind conditions on Inexpressible Island

The impact of changes in SLP in the Ross Sea and Victoria Land coast, discussed above, are also evident in the measurements from Manuela AWS station (Fig.4), placed on the southern part of Inexpressible Island. It is frequently affected by the katabatic winds entering the bay through the Reeves and Priestley glaciers. Thanks to its location in the transition zone between the Terra Nova Bay and Nansen Ice Sheet it provides a valuable source of information about katabatic flow properties before it enters the Ross Sea. Between 18–25 of September 2012 the prevailing direction of the wind was west northwest, which is typical for katabatic wind regimes in this region (Davolio & Buzzi, 2002). The wind speed varied from 5 m/s to 39 m/s, preceding the periods of polynya closing and opening. The katabatic flow coming off the slopes of Transantarctic Mountains has the properties of the air in the interior of the continent, it is dry and cold. Wind speeds above 20 m/s oberved by Manuela AWS coincide with an air humidity decrease below 40% and a temperature drop of a few degrees–down to -35^{o}C. The closing of the polynya on the 23rd corresponds to significant change in the air properties on the Inexpressible Island. For a short period of time the wind speed was below 5 m/s, air humidity above 80% and air temperatures increased to -20^{o}C, , revealing a reduced influence of continental air at this site. Atmospheric pressure changes observed at Manuela AWS are in agreement with MERRA reanalysis results. On the beginning of analysed period, between 18-20 September atmospheric air pressure remains low due to the cyclone dominance in the Ross Sea, then increases in response to the influence of an anticyclone coming from north east, to finally decrease because of the formation of a new mesocyclone offshore.

4 The atmosphere–surface coupling during different stages of polynya development.

The Aerosonde UAS flight days coincide with different phases of polynya development. The first stage, found on 18 and 19 September, corresponds to the early phase of polynya expansion–an opening mode, with increasing intensity of the katabatic wind. While on the days of 22 and 25 of September the TNBP encompasses a considerable part of the bay and weakening of the flow intensity is observed, followed by the polynya shrinking. Both periods differ in terms of the vertical and horizontal extent of polynya influence on the ABL. In the following paragraphs the atmosphere–surface coupling during the measurements is studied in detail, with additional description of atmospheric and surface conditions from the days between UAS Aerosonde flights.

4.1 18 and 19 September 2012

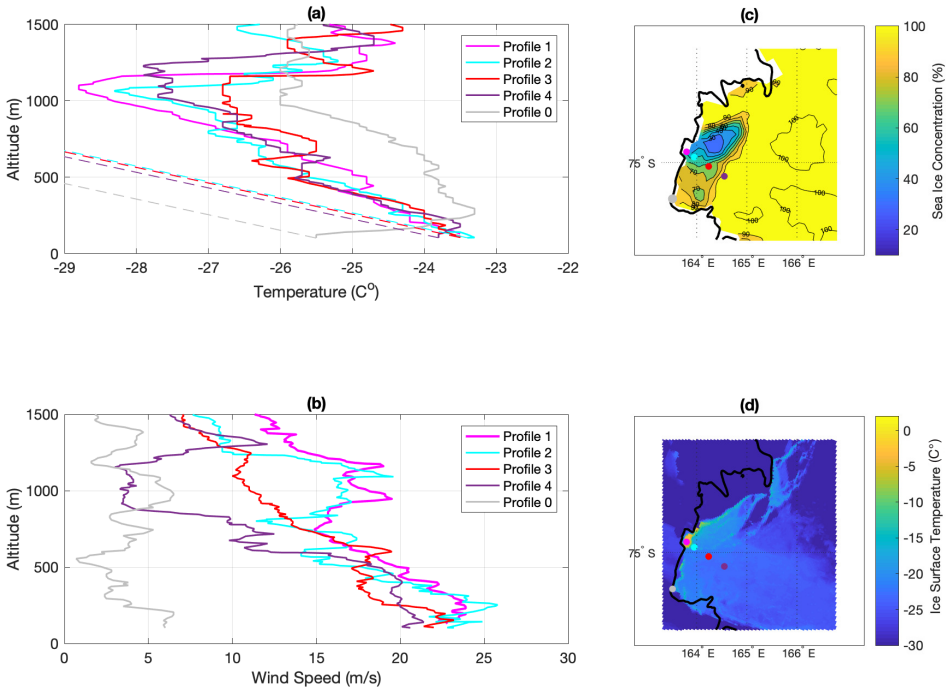

Figure 5. Vertical measurements of temperature (a) and wind speed (b), with the locations of UAS Aerosonde flights plotted on the map of SIC (c) and IST (d) on 18th of September 2012. Dashed lines on the temperature plot represent dry adiabatic lapse rate.

On 18 September the polynya is small, with only a narrow streak of very low sea ice concentrations (<40%) along the Nansen Ice shelf (Fig.5). Further offshore the IST image reveals several cracks in the compact sea ice, which on the following day breaks into floes and makes room for the expansion of the polynya. The wind speed on 18 September exceeded 20 m/s near the ice shelf edge with a small decrease further offshore (Fig.5). Favorable synoptic conditions in the form of large pressure gradient and isobars parallel to Victoria Coast (Fig.3), resulted in an increase of wind speed to nearly 30 m/s near the coast of TNB in the subsequent profiles from 18 September (Fig.6) and 35 m/s in all the flights from 19 of September (Fig.7). While on the first analyzed day the temperatures varied from -28°C to -23°C offshore, on the following day the air in the katabatic flow cooled down to -35°C in all profiles.

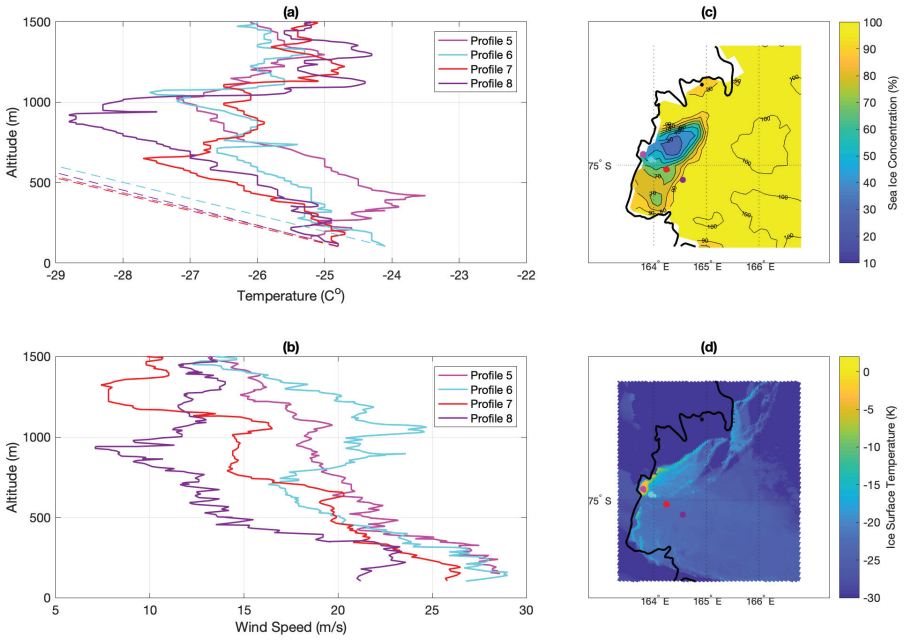

Figure 6. UAS Aerosonde measurements repeated 3.5 hours after then the profiles in Fig.5. Labeled as in Fig.5.

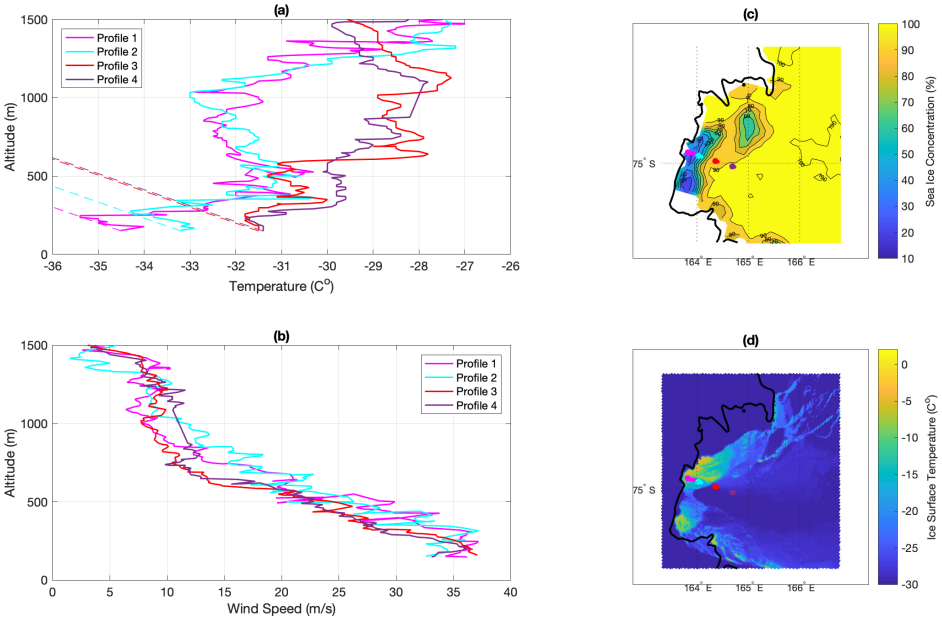

Figure 7. UAS Aerosonde measurements from 19th of September 2012. Labeled as in Fig.5.

The convection develops, extending up to the level of UAS flight (Fig.7) ∼100 m, as indicated by the nearly dry adiabatic lapse rate of temperature profiles. The depth of convection increases up to approximately 150 m height in the subsequent downwind profiles of 18 September and more than 200 m on the consecutive day, with the top of

the convective layer marked by an inversion. The formation of the convective boundary layer is a result of large temperature difference between the surface of open, or covered by thin layer of ice, water and the continental Antarctic air. Due to this temperature difference a considerable amount of heat is released from the ocean to the atmosphere which is then advected further downwind by the ongoing, intensive flow. In consequence, the remnant of the convective layer is also present over the areas of high SIC and compact sea ice (profiles 3 and 4; Fig.7).

Small changes of temperature with the distance offshore, observed on 18 of September (Fig.5 (a) and 6 (a)), indicate little transfer of heat between the ice covered ocean and the atmosphere due to low IST and high SIC. Meanwhile, downwind decrease of wind speed suggests momentum loss from the atmosphere to the ice and ocean surface, which results in the transport of ice away from the coast and waves generation in the open water of the polynya. In consequence, on the 19 of September the polynya is larger and the ABL properties change. While the upstream profiles show the development of convection (Fig.8, profile 2) and downstream warming (Fig.8, profile 1, 3) the profiles located over areas of thicker ice and lower IST show air cooling from the surface (Fig.8, profile 3, 4). Whereas, the overall higher temperatures in the latter profiles (5–8) from 19 September could be the result of warming from the polynya or a change in the upstream conditions. Considering, that upstream profile from Figure 9 (profile 5) is warmer than the corresponding, preceding profile from Figure 8 (profile 1) and they are both located over open water area, this shift in atmospheric conditions probably reflects some changes of temperature over the continent.

It is worth to have a look at profile 0 (Fig.5) located on the edge of the ice shelf, beyond the influence of the katabatic flow. It provides a view into the atmosphere in the area barely affected by extremely strong downslope winds. Due to an imbalance between the outgoing longwave radiation and the downwelling solar and longwave radiation the surface based inversion is present there, as is common in the polar regions. Temperature increases till the altitude of 300 m and then gradually decreases with height, while wind speed fluctuates around 5 m/s in the whole profile. In general, compared to other profiles the difference is explicit, confirming the importance of katabatic wind events in the local and regional atmosphere dynamics.

4.2 22 and 25 September 2012

The Manuela AWS station measurements (Fig.4) and satellite images indicate that on the 19 and 20 of September 2012 the wind remained strong and the polynya area expanded farther into the bay. The atmospheric pressure on the Inexpressible Island increased due to an extending influence of an anticyclone incoming into the region from northwest–signaling the closing of the polynya on the 23 of September. On the following day, 24 of September, the polynya opens again, partially in consequence of the anticyclone weakening and the decreasing pressure in the eastern part of Ross Sea. However, on 25 the synoptic situation changes again and the air pressure on the Inexpressible Island starts to increase, again indicating the closing of the polynya on the following day. Therefore, the situations on both 22 and 25 of September 2012 are to some extent similar, as they are both associated with large areas of low SIC and are followed by considerable weakening of the katabatic flow.

The flights on the 22 and 25 of September included vertical profiles along the path of the katabatic flow (Figs. 8–13). Throughout those days the profiles in Figures 8 to 13 are roughly aligned with the wind direction, so the winds shift from westerly to northwesterly to southwesterly. A portion of strong wind in the area adjacent to Drygalski Ice Tongue, indicates the increasing importance of the David Glacier's contribution to the flow. Each of the analyzed flights was proceeded by at least 24 hour of polynya remaining open over a large portion of the Terra Nova Bay. Consequently the continen-

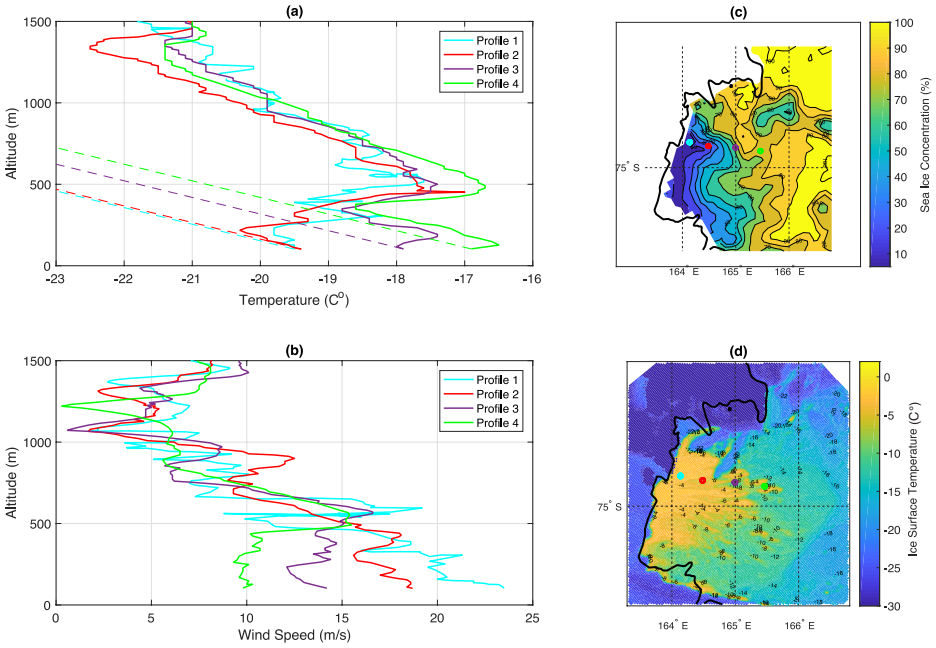

Figure 8. UAS Aerosonde measurements from 22nd of September 2012. Labeled as in Fig.5.

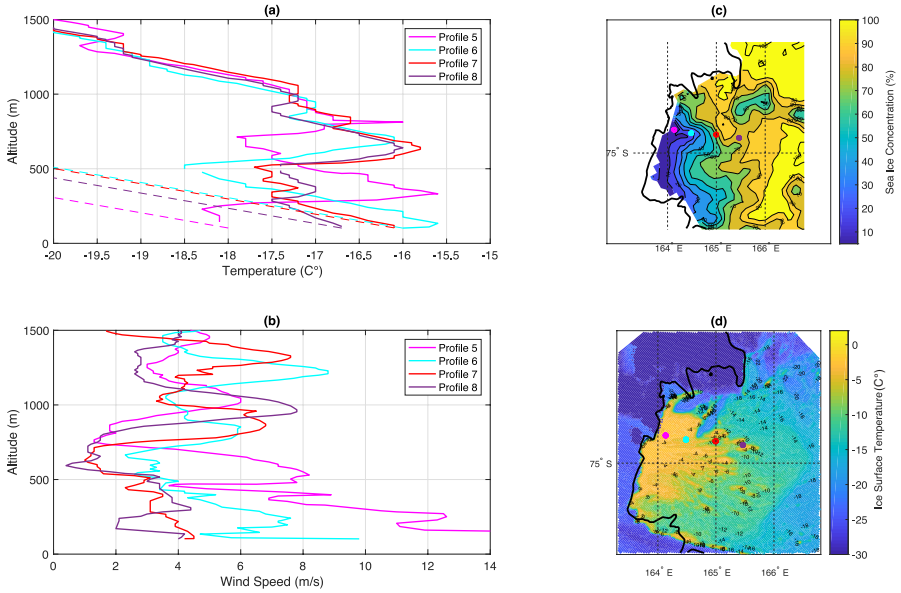

Figure 9. UAS Aerosonde measurements repeated 5 hours after the profiles in Fig.8. Labeled as in Fig.5.

tal air warmed up significantly as it passed over the TNBP and the convection, in some cases, is exceptionally strong. In the center of the katabatic flow, on 22 of September the temperatures downwind reached -15°C with convection extending up to 600 m altitude (profile 11, Fig.10), in comparison to the profile closer to the shore: -19°C and the capping inversion at 200 m (profile 9, Fig.10). The exceptionally strong convection near the

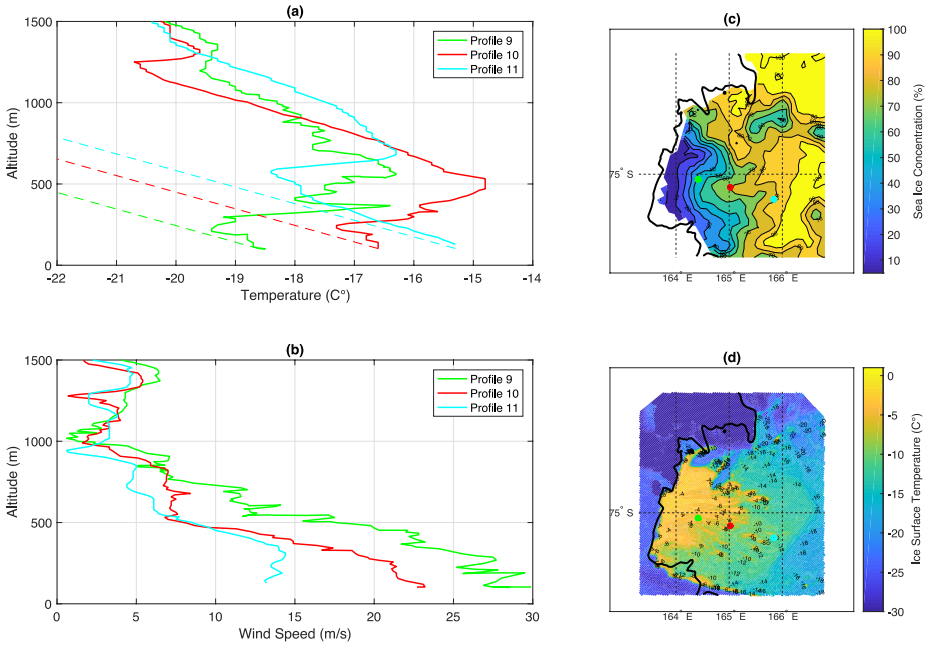

Figure 10. UAS Aerosonde measurements from 22nd of September 2012. Labeled as in Fig.5.

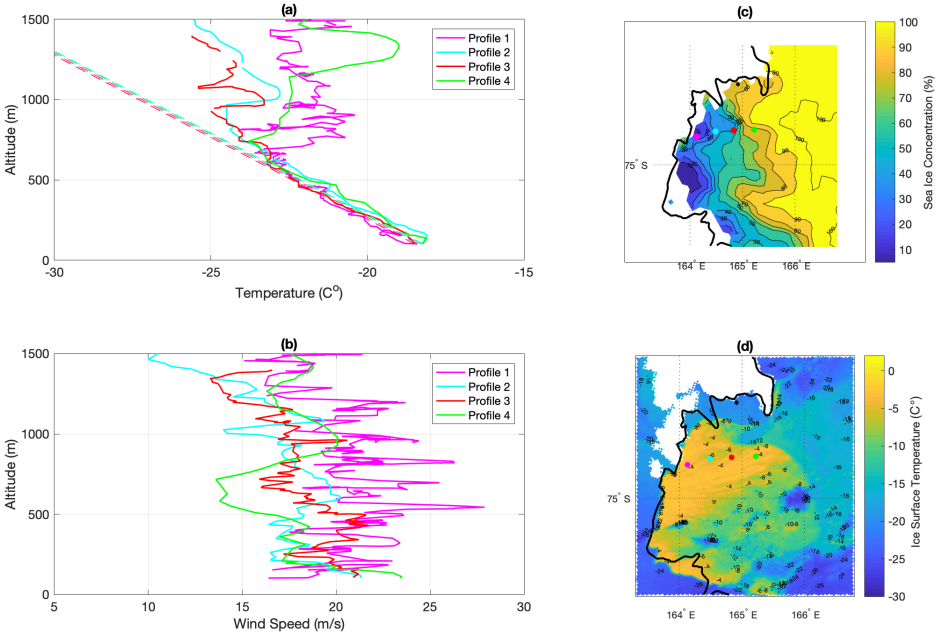

Figure 11. UAS Aerosonde measurements from 25th of September 2012. Labeled as in Fig.5.

edge of compact sea ice is a result of decreased wind speed, vigorous convective mixing and advection of heat from the area of lowest SIC near the edge of Nansen Ice Sheet. Another two flights done on that day took place to the north of the main path of the katabatic flow (Figs.8,9). Similar pattern of atmosphere warming and flow strength weakening is observed there as in aforementioned profiles, but with smaller convection height of 400 m in the most downwind profile (Fig8). The same flight pattern was repeated a

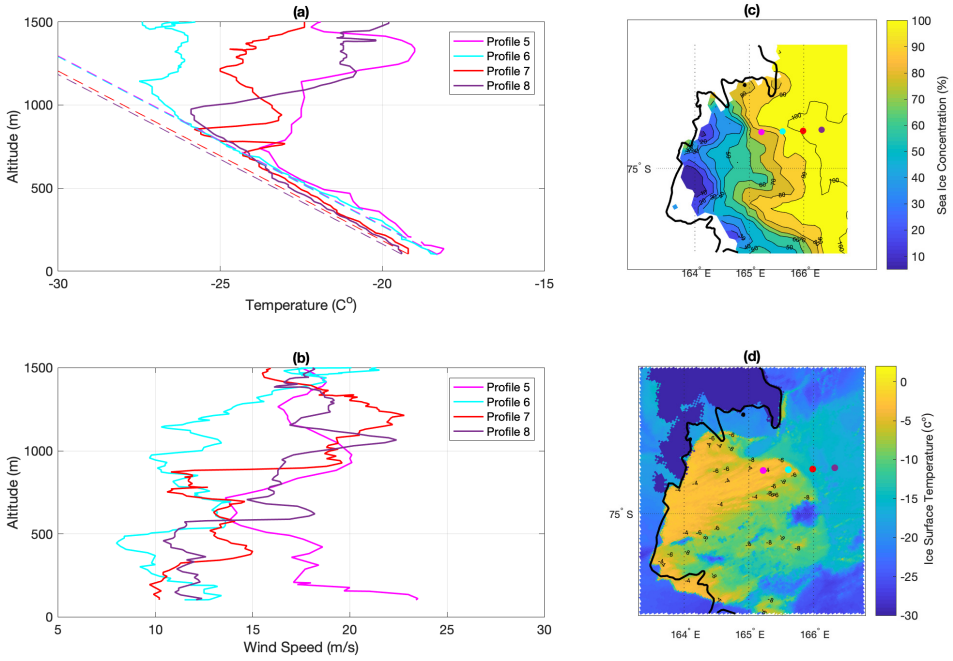

Figure 12. UAS Aerosonde measurements from 25th of September 2012. Labeled as in Fig.5

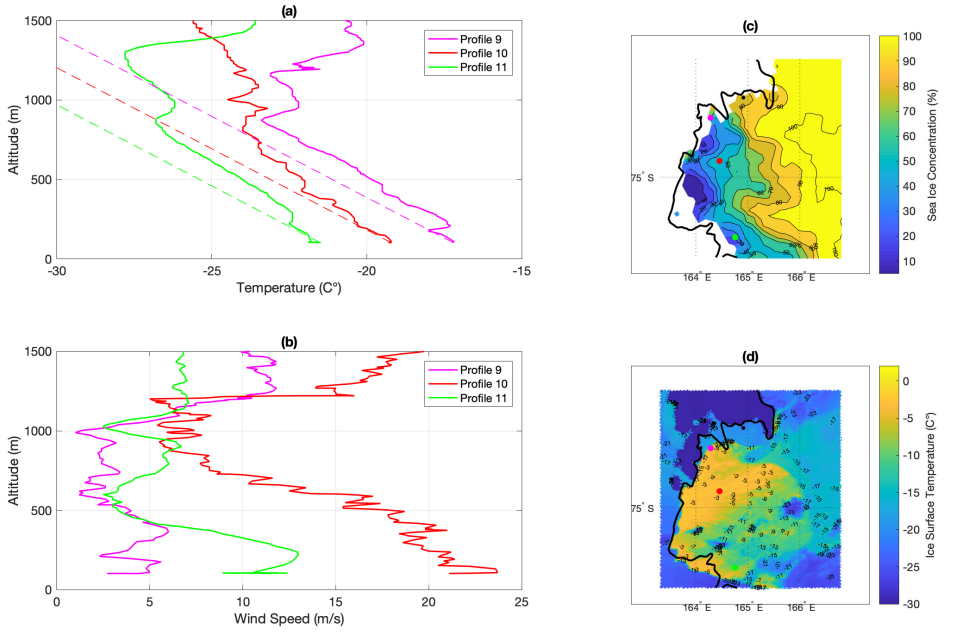

Figure 13. UAS Aerosonde measurements from 25th of September 2012. Labeled as in Fig.5

few hours later, when the intensity of the flow decreased even further (Fig9), likewise the transport of sea ice. Hence, the temperature on the lowest flight level increased and convection weakened due to changes in surface conditions. The decrease of wind speed leads to polynya closing on the following day.

On the 25 of September the polynya is opened again. In contrast to the measurements from 3 days back, the upward air motions on the verge of the main path of the katabatic flow are very strong in all the profiles, with convective boundary layer height of 700 m upwind (Fig.11) and 1000 m downwind (Fig.12). Deeper convective layer reflects the colder temperatures aloft on this day and thus the warm air at the surface is able to mix to deeper height that on the 22 September. Furthermore, temperature profiles downwind and upwind differ only slightly, due to very deep convective boundary layer and resulting extensive heating of the atmosphere. In fact, the heat gained from the surface upstream is spread over a larger mass of air and thus the downstream warming is less pronounced. Meanwhile, gradual cooling in the downstream direction, far from the shore, found in Figure 12 (a), is a result of reduced heat exchange between the atmosphere and the surface over more consolidated sea ice.

Another set of vertical UAS Aerosonde flights involved 3 profiles located across Terra Nova Bay, in a region with SIC below 40% (Fig.13). These profiles sample the weaker flow at the southern and northern edge of the katabatic flow (profiles 9 and 11) and stronger one near the core of the offshore flow (profile 10). In profiles 9 and 11 the convective boundary layer extends to 200 m of altitude, the elevated inversion is found at ∼900 m and the wind speeds are weak. The katabatic flow remains strong only in profile 10, which also has more vigorous convection with a convective boundary layer extending to 500 m. In general, the weakening of the katabatic flow influence across the bay (profile 9 and 11) indicates the shrinking of the polynya in the following hours.

The differences between the ABL warming and the convective boundary layer height are to some extent a consequence of higher/lower SIC and IST in the profile's locations. However, the events before the days of UAS Aerosonde flights may also be taken into account. Through the examination of Manuela AWS measurements (Fig. 4) it can be seen that polynya opening on the 22 of September is preceded by several periods of strong winds (>20 m/s), low temperatures and low humidity. While those conditions are typical for an inflow of continental, Antarctic air associated with katabatic winds, the significant expansion of the polynya starts on 21 and 22 of September when the flow speed exceeded 30-35 m/s. In comparison, the days before 25 of September are in general calmer in terms of wind speed but include a short event of exceptionally strong downslope flow of 35 m/s, followed by significant polynya opening. Therefore, while strong winds (>20 m/s) maintain the area of open water near the Nansen Ice Shelf, the short, exceptionally strong wind events are required for the polynya development far offshore.

5 Validation of AMPS results

The following analysis focuses on the UAS Aerosonde profiles, examined in section 4 and Manuela AWS observations from the period of 18–25 September 2012. The nearest points on the AMPS model grid to the locations of the UAS Aerosonde measurements are found and the vertical profiles from those points are compared with the observations. The AMPS model capability to simulate vertical and temporal changes of temperature and wind speed are examined. The aim of presented study is to validate the AMPS potential to reproduce the vertical properties of the atmosphere (temperature and wind) during different stages of polynya development, along with temporal changes of katabatic wind intensity on the Inexpressible Island.

5.1 UAS Aerosonde observations and AMPS model vertical changes of temperature and wind speed.

The following statistics are calculated for every UAS Aerosonde and matching AMPS model vertical profiles, for both temperature and wind speed: RMSE (Root Mean Squared Error), Pearson's correlation coefficient (Corr. coef.) and MBE (Mean Bias Error) (Tab.1). AMPS results for the 18 of September underestimate wind speed, especially in the pro-

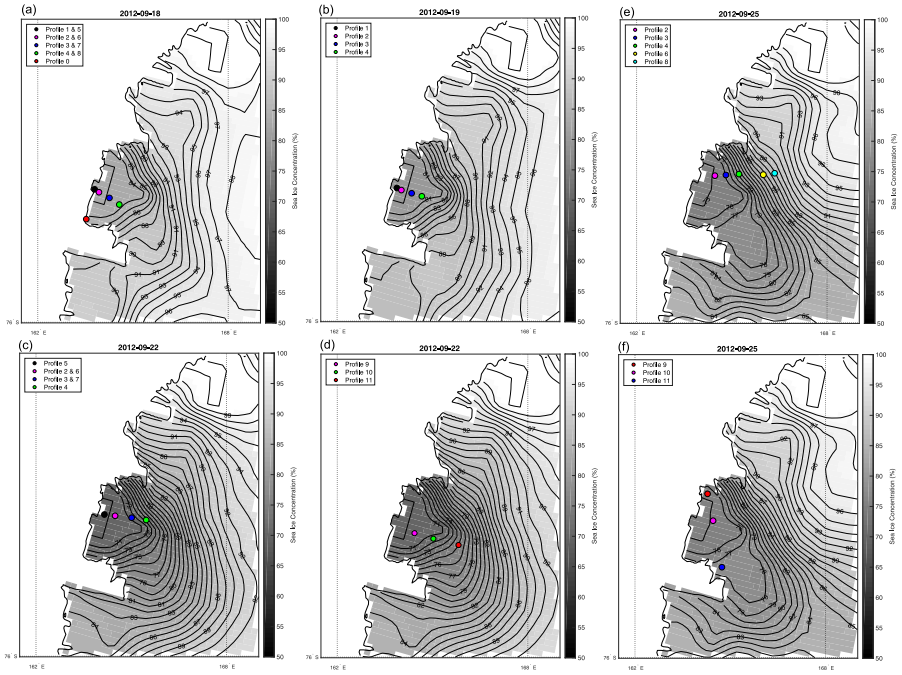

Figure 14. Location of the UAS Aerosonde profiles with maps of AMPS sea ice concentration.

Table 1. Statistics for the comparison of AMPS results and UAS Aerosonde profiles. T- temperature, WS- wind speed.

Date and profile number	RMSE (T)(°C)	Corr. coef. (T)	MBE (T)(°C)	RMSE (WS) (m/s)	Corr. coef. (WS)	MBE (WS) (m/s)
18 Sep. Profile 1	2.65	-0.37	1.09	6.52	0.82	-2.26
18 Sep. Profile 2	2.58	-0.39	1.34	6.36	0.85	-1.13
18 Sep. Profile 3	2.51	-0.42	0.59	5.25	0.96	-1.40
18 Sep. Profile 4	2.19	0.13	1.26	8.87	0.88	-7.28
18 Sep. Profile 5	0.91	0.43	-0.18	11.41	0.94	-11.19
18 Sep. Profile 6	1.40	0.49	0.96	11.27	0.57	-7.40
18 Sep. Profile 7	0.91	0.21	-0.22	11.43	0.53	-10.41
18 Sep. Profile 8	1.22	0.41	-0.53	7.92	0.60	-7.33
18 Sep. Profile 0	1.51	0.86	1.08	1.66	0.32	-0.83
19 Sep. Profile 1	2.91	-0.72	-0.00	4.20	0.96	-2.99
19 Sep. Profile 2	2.87	-0.78	0.09	5.99	0.92	-4.46
19 Sep. Profile 3	1.86	0.00	-0.85	4.98	0.98	-4.50
19 Sep. Profile 4	1.54	-0.16	-0.70	6.98	0.97	-6.51
22 Sep. Profile 2	1.44	0.80	0.65	4.12	0.92	-0.35
22 Sep. Profile 3	0.83	0.93	-0.43	6.35	0.80	0.02
22 Sep. Profile 4	0.84	0.90	-0.40	7.84	0.61	1.55
22 Sep. Profile 5	0.71	0.92	0.22	4.46	0.83	-3.25
22 Sep Profile 6	1.00	0.76	-0.45	4.43	0.82	2.78
22 Sep. Profile 7	1.71	0.43	-0.71	4.38	0.20	2.30
22 Sep. Profile 8	0.89	0.83	0.25	7.93	-0.34	4.15
22 Sep. Profile 9	1.33	0.90	-1.05	3.63	0.97	-2.85
22 Sep. Profile 10	1.11	0.83	0.09	5.46	0.88	-2.06
22 Sep. Profile 11	1.25	0.62	-0.04	1.80	0.96	1.05
25 Sep. Profile 2	3.22	0.85	-2.94	5.43	0.60	2.18
25 Sep. Profile 3	2.50	0.93	-2.41	6.82	0.75	3.83
25 Sep. Profile 4	4.09	0.53	-3.87	6.18	0.29	-5.08
25 Sep. Profile 6	2.87	0.87	-2.78	9.12	-0.48	-7.64
25 Sep. Profile 8	4.60	0.35	-4.21	9.93	-0.45	-8.83
25 Sep. Profile 9	1.44	0.77	-0.92	17.27	-0.57	14.55
25 Sep. Profile 10	2.98	0.50	-2.58	6.86	0.41	-0.85
25 Sep. Profile 11	2.49	0.39	-1.60	4.68	0.63	-4.08

files located further away from the shore (MBE<-7 m/s; Tab.1 18 Sep. Profile 4) and the ones completed few hours later (Tab.1; 18 Sep. Profile 5–8). In profiles 1-3 (Tab.1; 18 Sep. Profile 1–3), up to the height of ∼600–800 m, simulated wind speeds are higher than measured ones but they decrease more rapidly with height which leads to signif-

icant negative bias (>-5 m/s) at the highest altitudes (Fig.15, (b)). On the next day the vertical changes of wind speed in the ABL are well simulated, with greater values of the Pearson's Corr. Coef.(∼0.9) and lower errors (RMSE <6 m/s, MBE>-7 m/s). When it comes to temperature, for the upwind profile locations, AMPS simulates a strong inversion, and thus is negatively correlated with the observations (Corr. coef.<-0.3; Tab.1; 18 Sep. Profile 1–3). In the downwind profiles (Tab,1; 18 Sep. Profile 4) and the ones carried out ∼3.5 hours later (Tab. 1; 18 Sep. Profile 5–6) the AMPS inversion is absent and the bias between UAS Aeroronde measurements and AMPS model output decreases (on average: MBE<1 m/s, Corr. coef.>0). On the other hand, on the following day the values of MBE for temperature are even smaller, although the linear correlation is negative (Corr. coef.<0; Tab.1; 19 Sep. Profiles 1–4). Such results are a consequence of decreasing modeled temperatures above ∼ 800 m, in comparison to observed ones which gradually increase (Fig.15, (c)).

In the next days of UAS Aerosonde flights, 22 and 25 of September, the polynya encompassed a significant portion of Terra Nova Bay. Observations indicate that throughout the 22 of September the intensity of katabatic winds decreased in time. This weakening of the katabatic flow is less pronounced in model results (Fig.15,(f)), as indicated by lower values of Corr. Coef. (0.61 in Profile 4,0.2 in Profile 7 and -0.34 in Profile 8) and higher RMSE (>4 m/s) (Tab.1; 22 Sep. Profiles 5–8). A similar situation is found on 25 of September, when the modeled upstream air flow is faster (Fig.15,(h); MBE>2m/s; Tab.1; 25 Sep. Profiles 2-3). In comparison, further offshore the AMPS underestimates wind speeds (MBE<0), which leads to significant differences and negative correlation between modeled and observed values (Corr. Coef. of -0.48,-0.45 and -0.57 for profiles 6, 8, 9, Tab.1; 25 Sep.). Statistics for Profiles 9–11 from 25 of September (Tab.1; 25 Sep.) indicate that wind speed in the northern part of TNBP is overestimated (MBE of 14.55 m/s) and underestimated in the central and southern part (MBE<0), thus the simulated katabatic flow position is slightly shifted in the model results. When it comes to temperature the statistics show good linear correlation (Corr. Coef., on average >0.6; Tab.1; Profiles 22 Sep. Profiles 2–11 and 25. Sep Profiles 2–11), thus signaling small differences between modeled and observed values. Nonetheless, on 22 of September the AMPS results include weaker convection and stronger inversion layers than measured by UAS Aerosonde, beginning at the height of ∼50–100 m (Fig.15,(e)). At the altitude of approximately 600 m both modeled and observed vertical changes of temperature are analogous in all profiles from this day, with an underestimation in AMPS results (MBE<-2°C). On 25 of September the model simulates colder temperatures, with negative bias of approximately 2–3°C. However, the vertical variations of temperature with height are in good agreement, as both profiles take similar shape (Fig.15(g)) and involve strong convection up to a few hundred meters. Larger values of both RMSE and MBE for profiles 4 and 8 (RMSE>4 °C and MBE<-3.5 °C; Tab.1; 25 Sep.) are a consequence of more intensive warming of the atmosphere above 1000 m in the UAS Aerosonde measurements.

On the whole, the average values of RMSE and MBE for all analyzed profiles are 1.91°C and -0.37°C for temperature and 6.45 m/s and -2.75 m/s for wind speed. Therefore, both atmospheric properties are slightly underestimated. However, most of the discrepancies between the modeled and observed values originate in the lowest layers of the ABL, especially when it comes to temperature. The AMPS results in most of the profiles include inversions which are associated with much larger SICs incorporated into the model (Fig.14) than the ones caught by AMSR2 sensor (Figs.5–13). Furthermore, the modeled katabatic flow seems to be slightly shifted to the north, in comparison to observed one.

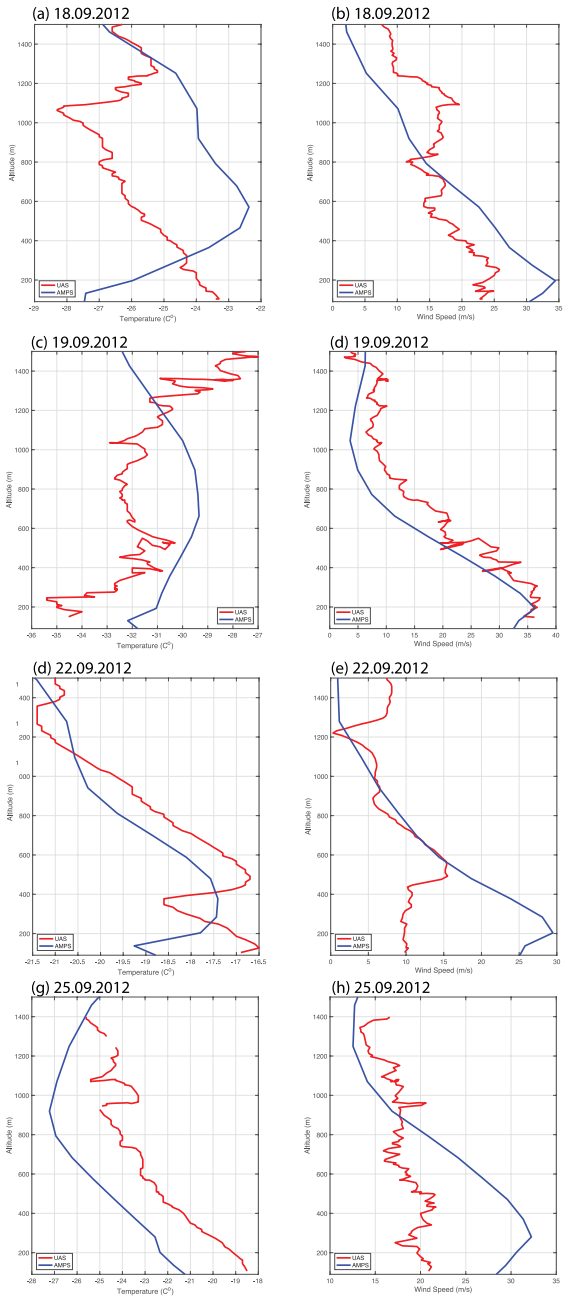

Figure 15. Exemplary profiles from UAS Aerosonde observations and AMPS model results. (a–b) Profile nr. 2, 18.09.2012.(c–d) Profile nr. 2, 19.09.2012. (e-f) Profile nr 5, 22.09.2012. (g–h) Profile nr. 3, 25.09.2012.

5.2 Manuela AWS and AMPS model time series for temperature and wind speed.

In addition to the vertical comparison of AMPS and UAS profiles of temperature and wind speed a time series for the nearest model grid point to Manuela AWS are compared with the measurements from the station for the period between 18–25 September.

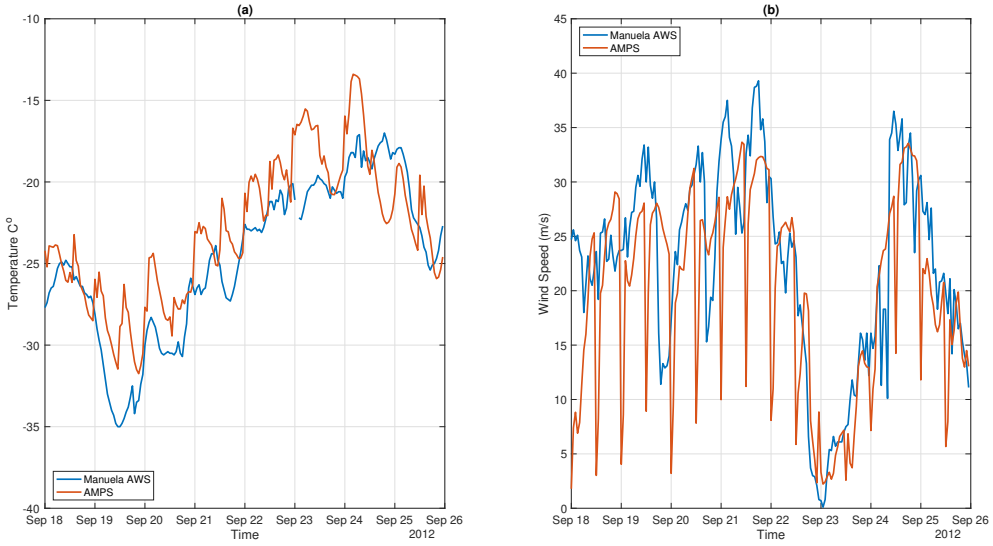

Figure 16. Observations from Manuela AWS station and model results from the nearest point to Manuela AWS location for (a) temperature and (b) wind speed between 18 and 25 September 2012.

The same statistics as in the previous section are calculated to assess the correlation between modeled and observed values (Tab.2). The value of corr.coef . indicates that the temperature variations with time are better simulated by AMPS than wind speed (0.86 and 0.66, respectively), while RMSE and MBE reveal overestimation of temperature and underestimation of wind speed (0.86 and 0.66, respectively). To a large extent those incompatibilities are a consequence of model reinitialization times of 00 and 12 UTC from a coarser resolution that doesn't adequately capture the katabatic flow in Terra Nova Bay, as seen in Fig.16). In consequence, the AMPS model output involves daily changes of wind speed from 5 m/s to almost 30 m/s. To the advantage of AMPS, apart from reinitialization times the general pattern of temperature and wind speed changes throughout the studied period is well simulated, in particular–intensive katabatic flow on the 18–22 and 25 September and its absence on 23 of September.

Table 2. Statistics for the comparison of AMPS results and AWS Manuela observations between 18 and 25 September 2012. T- temperature, WS- wind speed.

18-25 Sep. 2012	RMSE (T) (°C)	Corr. coef. (T)	MBE (T) (°C)	RMSE (WS) (m/s)	Corr. coef. (WS)	MBE(WS) (m/s)
Manuela AWS	2.90	0.86	1.63	8.05	0.66	-2.6

6 Discussion

This study demonstrates the influence of the katabatic flow on the atmospheric and surface conditions in the Terra Nova Bay and how it is, to a certain degree, governed by sea level pressure changes in the Ross Sea region. UAS Aerosonde measurements provide important information on the development of convective boundary layer, wind speed changes with the distance offshore and ABL properties in different parts of the bay. Together with surface SIC and IST datasets they reveal the complexity of polynya development and transformations caused by forcings of various temporal and spatial scales.

UAS Aerosonde measurements between 18–25 September, along with MERRA sea level pressure data, demonstrate that large pressure difference between the Transantarctic Mountains and the Ross Sea contributes to the acceleration of wind speed to 30–35 m/s and the preservation of their strength after passing over the polynya. However, despite the exceptional intensity of the flow the expansion of the polynya depends also on the duration of such events. Moreover, our analysis points out that surface and atmospheric conditions in the preceding days also play a role in TNBP development. The analysis above indicates that a large polynya exceeding the area of 2000 km^2 is more probable to develop when: wind speeds above 20 m/s persists for several days in advance; polynya encompassed a large portion of Terra Nova Bay within few days back and current wind speed exceeds 30–35 m/s. Furthermore, 18 and 19 of September can be recognized as the days of katabatic flow intensification and the beginning of sea ice breakup. This period is characterized by wind speeds increasing from 20 to 35 m/s, low temperatures (<-20°C) and only slight air mass modifications with the distance offshore due to limited heat exchange between the atmosphere and ice covered surface. Whereas on 22 and 25 the polynya covers a large portion of Terra Nova Bay and the ABL is well mixed, warm and convective with decreasing wind speed and temperature increase in the downwind direction. Therefore, the flow of extremely cold, dry winds results in the development of convective boundary layer, very shallow at first but growing in height through the consecutive days of UAS Aerosonde flights and polynya expansion. In fact, the longer the polynya is opened and the the closer to the ice edge the measurements took place– the more intensive is the convection. The weakening of the flow is accompanied by a large increase of temperature, from the ~ -35°C when the wind speeds exceeded 35 m/s to ~ -19°C when the flow slowed down to 20 m/s. The termination and initiation of extreme wind can occur within several hours. In general, although UAS Aerosonde flights encompassed only several days they provided a comprehensive view on different stages of polynya development and a valuable dataset for the validation of model results.

Results of the presented analysis include features and processes associated with TNBP changes that are also found in a number of modeling studies. Different stages of polynya development are identified by Petrelli et al. (2008), while the importance of duration and certain threshold of katabatic flow strength necessary for the expansion of the TNBP have been mentioned by, among others, Ciappa et al. (2012); Yoon et al. (2020). The opening and closing of the polynya occurs on very short timescale and the weakening of the winds results in a rapid reduction of polynya size, as stated by Bromwich and Kurtz (1984). As in the studies of Gallée (1997); Dare and Atkinson (1999); VanWoert (1999) the atmosphere warms with the distance from the ice shelf and as the air is constantly advected downwind–the maxium height of mixed layer is found there. The acceleration of wind at the ice edge, found in modeling results (Gallée, 1997; Dare & Atkinson, 1999), is hard to distinguish in the UAS Aerosonde observations. Even when the polynya encompasses a significant portion of the bay (22 and 25 September) the strongest wind persists near the ice shelf and weakens with the distance offshore. Numerical modeling studies of e.g. Gallée (1997); Dare and Atkinson (1999) find the maximum wind speed at the atltitude of 150 or 400 m, while presented research indicates that highest wind speed occurs between ∼100–400 m above the surface, however the exact height depends on the stage of polynya development, intensity of the katabatic flow and surface conditions.

Moving on to the analysis of AMPS forecasts for the days between 18–25 September 2012. The model simulates well the temporal changes of temperature throughout the analyzed period, including the extremely cold flow off the Transantarctic Mountains and its absence on 23 of September. The large fluctuations of wind speed found in the AMPS model results ,not present in Manuela AWS observations, are probably caused by the the errors associated with model reinitialization from coarser resolution modelat 00 and 12 UTC. Those fluctuations may also be the reason behind the errors reported in Tab.1. Apart form those drawbacks the model resolves well the advancement of the extreme winds, particularly in the upwind areas. The spatial distribution of the katabatic flow is only

slightly flawed as it is somewhat more shifted to the north–west direction compared to observations, probably due to dominating, northern direction of mesoscale wind and the model assumption that the flow from Reeves Glacier is predominant. The errors associated with the location and temporal changes of wind speed affect also the accuracy of temperature predictions, mostly due to slightly different spatial distribution of cold, dry air. Furthermore, the SICs incorporated into the model (Fig.14) are exaggerated in comparison to the ones reported by AMSR2 sensor (Fig. 5–13). In consequence the lowest layers of the ABL in the AMPS forecasts include low level inversions and colder temperatures than the ones observed by UAS Aeorosonde. Overall, such misinterpretations of the ABL stability lead to errors in the predictions of atmospheric properties important for aircraft operations, like vertical motions and momentum fluxes. Nevertheless, despite those shortcomings the AMPS model produces fairly useful forecasts for the analyzed region, particularly in regard to the upwind conditions in the Terra Nova Bay. This study also emphasizes the importance of observations in model validation and the directions in which AMPS should improve to provide better forecasts for aerial missions.

Due to data availability in the form of satellite images the majority of TNBP studies focused on polynya size and the relationship between its size and the strength of katabatic winds. Presented research indicates that full understanding of those processes requires a broader view, which takes into account synoptic forcing, flows from different glaciers and atmospheric–surface coupling. UAS Aerosonde measurements, satellite SIC and IST data along with the synoptic overview of mesoscale atmospheric conditions, from reanalysis data, enable an identification of the factors leading to polynya opening and expansion. Therefore, the need for more observations and field campaigns for models validation and development is unambiguous and requires attention of scientific community.

Acknowledgments

This work was funded by the Polish National Science Centre grant No. 2019/32/T/ST10/00171 "Submesoscale atmospheric boundary layer processes over inhomogenous sea ice.". The data files for each analyzed flight are available from the United States Antarctic Program Data Center (`http://gcmd.nasa.gov/getdif.htm?NSF-ANT10-43657,doi:10.15784/600125`).

References

Adams, S., Willmes, S., Heinemann, G., Rozman, P., Timmermann, R., & Schröder, D. (2011). Evaluation of simulated sea-ice concentrations from sea-ice/ocean models using satellite data and polynya classification methods. *Polar Research*, *30*(1), 7124. doi: 10.3402/polar.v30i0.7124

Bromwich, D. (1989). An extraordinary katabatic wind regime at Terra Nova Bay, Antarctica. *Mon. Weather Rev.*, *117*(3), 688-695. doi: 10.1175/1520-0493(1989)117⟨0688:AEKWRA⟩2.0.CO;2

Bromwich, D., & Kurtz, D. (1982). Experiences of Scott's Northern Party: evidence for a relationship between winter katabatic winds and the Terra Nova Bay polynya. *Polar Record*, *21*(131), 137–146. doi: 10.1017/S0032247400004514

Bromwich, D., & Kurtz, D. (1984). Katabatic wind forcing of the Terra Nova Bay polynya. *J. Geophys. Res. Oceans*, *89*(C3), 3561-3572. doi: 10.1029/JC089iC03p03561

Bromwich, D., Otieno, F., Hines, K., Manning, K., & Shilo, E. (2013). Comprehensive evaluation of polar weather research and forecasting model performance in the Antarctic. *J. Geophys. Res. Atmos.*, *118*(2), 274-292. doi: 10.1029/2012JD018139

Bromwich, D., Steinhoff, D., Simmonds, I., Keay, K., & Fogt, R. (2011). Climatological aspects of cyclogenesis near Adélie Land Antarctica. *Tellus A: Dynamic Meteorology and Oceanography*, *63*(5), 921-938. doi: 10.1111/j.1600-0870.2011

.00537.x

Carrasco, J., & Bromwich, D. (1993, 07). Mesoscale cyclogenesis dynamics over the southwestern Ross Sea, Antarctica. *J. Geophys. Res.*, *98*, 12973-12995. doi: 10.1029/92JD02821

Cassano, J., Seefeldt, M., Palo, S., Knuth, S., Bradley, A., Herrman, P., ... Logan, N. (2016). Observations of the atmosphere and surface state over Terra Nova Bay, Antarctica, using unmanned aerial systems. *Earth Syst. Sci. Data*, *8*(1), 115–126. doi: 10.5194/essd-8-115-2016

Center, E. M. (2003). The GFS atmospheric model. *National Centers for Environmental Prediction Office Note*, *442*, 14.

Ciappa, A., Pietranera, L., & Budillon, G. (2012). *Observations of the Terra Nova Bay (Antarctica) polynya by MODIS ice surface temperature imagery from 2005 to 2010*. *Remote Sensing of Environment*, *119*, 158 - 172. doi: https://doi.org/10.1016/j.rse.2011.12.017

Dare, R., & Atkinson, B. (1999). Numerical modeling of atmospheric response to polynyas in the Southern Ocean sea ice zone. *J. Geophys. Res. Atmos.*, *104*(D14), 16691-16708. doi: 10.1029/1999JD900137

Davolio, S., & Buzzi, A. (2002). Mechanisms of Antarctic katabatic currents near Terra Nova Bay. *Tellus A*, *54*(2), 187-204. doi: 10.1034/j.1600-0870.2002.01290.x

Gallée, H. (1997). Air-sea interactions over terra nova bay during winter: Simulation with a coupled atmosphere-polynya model. *J. Geophys. Res. Atmos.*, *102*(D12), 13835-13849. doi: 10.1029/96JD03098

Key, J., Mahoney, R., Liu, Y., Romanov, P., Tschudi, M., Appel, I., ... Meade, P. (2013). Snow and ice products from Suomi NPP VIIRS. *J. Geophys. Res. Atmos.*, *118*(23), 12,816-12,830. doi: 10.1002/2013JD020459

Knuth., S., & Cassano, J. (2011). An Analysis of Near-Surface Winds, Air Temperature, and Cyclone Activity in Terra Nova Bay, Antarctica, from 1993 to 2009. *J. Appl. Meteorol. Climatol.*, *50*(3), 662-680. doi: 10.1175/2010JAMC2507.1

Knuth, S., Cassano, J., Maslanik, J., Herrmann, P., Kernebone, P., Crocker, R., & Logan, N. (2013, 02). Unmanned aircraft system measurements of the atmospheric boundary layer over Terra Nova Bay, Antarctica. *Earth System Science Data*, *5*. doi: 10.5194/essd-5-57-2013

Kurtz, D., & Bromwich, D. (1983). Satellite observed behavior of the Terra Nova Bay Polynya. *J. Geophys. Res. Oceans*, *88*(C14), 9717-9722. doi: 10.1029/JC088iC14p09717

Kurtz, D., & Bromwich, D. (2013). A recurring, atmospherically forced polynya in Terra Nova Bay. In *Oceanology of the antarctic continental shelf* (p. 177-201). American Geophysical Union (AGU). doi: 10.1029/AR043p0177

Lazzara, A., Weidner, G., Keller, L., Thom., J., & Cassano, J. (2012). Antarctic Automatic Weather Station Program: 30 Years of Polar Observation. *Bull. Am. Meteorol. Soc.*, *93*(10), 1519-1537. doi: 10.1175/BAMS-D-11-00015.1

Manzella, G., Meloni, R., & Picco, P. (1999). Current, temperature and salinity observations in the Terra Nova Bay Polynya area. In *Oceanography of the Ross Sea Antarctica* (pp. 165–173). Milano: Springer Milan.

Martin, J., Morris, K., Maksym, T., Kozlenko, N., & Tin, T. (2001). Autumn sea ice thickness, ridging and heat flux variability in and adjacent to Terra Nova Bay, Ross Sea, Antarctica. *J. Geophys. Res. Oceans*, *106*(C3), 4437-4448. doi: 10.1029/1999JC000021

Massom, R., Harris, P., Michael, K., & Potter, M. (1998). The distribution and formative processes of latent-heat polynyas in East Antarctica. *Annals of Glaciology*, *27*, 420–426. doi: 10.3189/1998AoG27-1-420-426

Minnett, P., & Key, E. (2007). Chapter 4 meteorology and atmosphere–surface coupling in and around polynyas. In W. Smith & D. Barber (Eds.), *Polynyas: Windows to the World* (Vol. 74, p. 127 - 161). Elsevier. doi: https://doi.org/

10.1016/S0422-9894(06)74004-1

Morelli, S., & Parmiggiani, F. (2013, Nov 12). Wind over Terra Nova Bay (Antarctica) during a polynya event: Eta model simulations and satellite microwave observations. *Eur. Phys. J. Plus*, *128*(11), 135. doi: 10.1140/epjp/i2013-13135-8

Pane, L., Feletti, M., Francomacaro, B., & Mariottini, G. (2004, 12). Summer coastal zooplankton biomass and copepod community structure near the Italian Terra Nova Base (Terra Nova Bay, Ross Sea, Antarctica). *Journal of Plankton Research*, *26*(12), 1479-1488. doi: 10.1093/plankt/fbh135

Parish, T., & Bromwich, D. (1989). Instrumented aircraft observations of the katabatic wind regime near Terra Nova Bay. *Mon. Weather Rev.*, *117*(7), 1570-1585. doi: 10.1175/1520-0493(1989)117⟨1570:IAOOTK⟩2.0.CO;2

Parmigianni, F. (2011). Multi-year measurement of Terra Nova Bay winter polynya extents. *Eur. Phys. J. Plus*, *126*(39). doi: 10.1140/epjp/i2011-11039-3

Petrelli, P., Bindoff, N., & Bergamasco, A. (2008). The sea ice dynamics of Terra Nova Bay and Ross Ice Shelf Polynyas during a spring and winter simulation. *J. Geophys. Res. Oceans*, *113*(C9). doi: 10.1029/2006JC004048

Powers, J., Kuo, Y., Bresch, J., Cassano, J., Bromwich, D., & Cayette, A. (2001). The Antarctic Mesoscale Prediction System. In *Sixth Conf. on Polar Meteorology and Oceanography* (p. 506-510). SanDiego,CA: Amer. Meteor. Soc.

Powers, J., Monaghan, A., Cayette, A., Bromwich, D., Kuo, Y., & Manning, K. (2003, 10). Real-time mesoscale modeling over Antarctica: The Antarctic Mesoscale Prediction System. *Bull. Am. Meteorol. Soc.*, *84*, 1533-1545. doi: 10.1175/BAMS-84-11-1533

Rienecker, M., Suarez, M., Gelaro, R., Todling, R., Bacmeister, J., Liu, E., ... Woollen, J. (2011). MERRA: NASA's Modern-Era Retrospective Analysis for Research and Applications. *J. Clim.*, *24*(14), 3624-3648. doi: 10.1175/JCLI-D-11-00015.1

Seefeldt, M., Cassano, J., & Parish, T. (2007). Dominant regimes of the Ross Ice Shelf surface wind field during austral autumn 2005. *JAMC*, *46*(11), 1933-1955. doi: 10.1175/2007JAMC1442.1

Spreen, G., Kaleschke, L., & Heygster, G. (2008). Sea ice remote sensing using AMSR-E 89-Ghz channels. *J. Geophys. Res. Oceans*, *113*(C2). doi: 10.1029/2005JC003384

Sprovieri, F., Pirrone, N., Hedgecock, I., Landis, M., & Stevens, R. (2002, 12). Intensive atmospheric mercury measurements at Terra Nova Bay in Antarctica during November and December 2000. *J. Geophys. Res.*, *107*, 4722. doi: 10.1029/2002JD002057

Tschudi, M., Riggs, G., Hall, D., & Romón, O. (2017). VIIRS/NPP Ice Surface Temperature 6-Min l2 Swath 750m, Version 1. *Boulder, Colorado USA. NASA National Snow and Ice Data Center Distributed Active Archive Center*. doi: doi:https://doi.org/10.5067/VIIRS/VNP30.001

VanWoert, M. (1999). Wintertime dynamics of the Terra Nova Bay polynya. *J. Geophys. Res. Oceans*, *104*(C4), 7753-7769. doi: 10.1029/1999JC900003

Vecchiato, M., Gregoris, E., Barbaro, E., Barbante, C., Piazza, R., & Gambaro, A. (2017). Fragrances in the seawater of Terra Nova Bay, Antarctica. *Sci. Total Environ.*, *593-594*, 375 - 379. doi: https://doi.org/10.1016/j.scitotenv.2017.03.197

Yoon, S., Lee, W., Stevens, C., Jendersie, S., Nam, S., Yun, S., ... Lee, J. (2020). Variability in high-salinity shelf water production in the Terra Nova Bay polynya, Antarctica. *Ocean Science*, *16*(2), 373–388. Retrieved from `https://www.ocean-sci.net/16/373/2020/` doi: 10.5194/os-16-373-2020

Yu, Y., & Rothrock, D. (1996). Thin ice thickness from satellite thermal imagery. *J. Geophys. Res. Oceans*, *101*(C11), 25753-25766. doi: 10.1029/96JC02242